

# Informed Graph Learning By Domain Knowledge Injection and Smooth Graph Signal Representation

Keivan Faghieh Niresi, Lucas Kuhn, Gaëtan Frusque, Olga Fink  
Intelligent Maintenance and Operations Systems (IMOS) Lab, EPFL, Switzerland  
{keivan.faghiehniresi, lucas.kuhn, gaetan.frusque, olga.fink}@epfl.ch

**Abstract**—Graph signal processing represents an important advancement in the field of data analysis, extending conventional signal processing methodologies to complex networks and thereby facilitating the exploration of informative patterns and structures across various domains. However, acquiring the underlying graphs for specific applications remains a challenging task. While graph inference based on smooth graph signal representation has become one of the state-of-the-art methods, these approaches usually overlook the unique properties of networks, which are generally derived from domain-specific knowledge. Overlooking this information could make the approaches less interpretable and less effective overall. In this study, we propose a new graph inference method that leverages available domain knowledge. The proposed methodology is evaluated on the task of denoising and imputing missing sensor data, utilizing graph signal reconstruction techniques. The results demonstrate that incorporating domain knowledge into the graph inference process can improve graph signal reconstruction in district heating networks. Our code is available at [github.com/Keiv4n/IGL](https://github.com/Keiv4n/IGL).

**Index Terms**—Graph learning, graph signal processing, graph signal reconstruction, smooth representation, domain knowledge

## I. INTRODUCTION

Spatial distribution of the collected data has emerged as an important property across a wide range of applications such as traffic data analysis [1], air pollution networks [2], and biological networks [3]. The intrinsic network characteristics of these datasets contain important insights into the connections and information between different entities across the network. Graphs are essential tools for representing the complex structures present in such data, as they provide flexible mathematical representations and can offer both analytical and visual foundations for understanding and interpreting large amounts of data. In recent years, there has been an effort to extend signal processing techniques to graphs, resulting in the emergence of the graph signal processing (GSP) field, which aims to improve the data representation on graphs [4], [5]. However, acquiring the underlying graphs for specific applications can be challenging, and constructing graphs based solely on network connectivity may not guarantee optimal results for certain subsequent tasks such as forecasting [6]. Therefore, it is crucial to infer a graph that effectively captures the structure of the data.

This research was funded by the Swiss Federal Institute of Metrology (METAS).

Graph inference is an ill-posed problem that aims to define the generative function most accurately describing the relationship between the learned graph topology and the observed data [7]. Sample correlation, Gaussian radial basis function kernel, and cosine similarity are among the most straightforward methods for capturing the similarity of data samples [8]. However, these methods are vulnerable to noise because they rely solely on observations and do not utilize an explicit prior or data model. Therefore, different approaches have recently been proposed for graph learning based on GSP [9]. These techniques allow for the direct extraction and inference of underlying graph structures from the data. Graph inference methods based on GSP can be categorized into global smoothness-based [10], [11], dictionary-based [12], and spectral template-based methods [13]. In this study, we focus on global smoothness-based methods for our proposed technique, ensuring its adaptability is preserved. This focus is motivated by the availability of scalable and efficient solvers within this category, which aligns well with the requirements of our proposed method which is mainly designed for large-scale sensor networks. Moreover, this type of method is explainable from both signal representation and statistical perspectives. For a comprehensive understanding of various methods, interested readers are encouraged to explore relevant literature [9], [14].

Although global smoothness-based methods have demonstrated competitive results in graph inference, they neglect the unique characteristics of the physical processes in networks derived from domain knowledge, potentially limiting their overall effectiveness and interpretability. To address this limitation, this study proposes a novel graph inference method that leverages the presence of domain knowledge. To optimize the graph inference task, we efficiently solve the optimization problem using the primal-dual splitting algorithm. We evaluate the effectiveness of our approach on the task of graph signal reconstruction for denoising and imputing missing sensor data in the district heating network. The key contributions of our work include:

- We propose a novel method for graph inference that leverages available domain knowledge.
- We present an efficient solution of the optimization problem through the use of a primal-dual algorithm.
- We validate the effectiveness of our proposed approach

through a case study on graph signal reconstruction, specifically in denoising and imputing missing data from district heating network sensors.

## II. PRELIMINARIES

### A. Graph Signal Processing

We consider a weighted undirected graph  $\mathcal{G} = (\mathcal{V}, \mathcal{E}, \mathbf{W})$ , where  $\mathcal{V}$ ,  $\mathcal{E}$ , and  $\mathbf{W}$  represent the sets of nodes, edges, and the adjacency matrix, respectively. The graph's topology is defined by the adjacency matrix  $\mathbf{W}$  of size  $n \times n$ , with  $\mathbf{W}(i, j)$  denoting the edge weight between vertices  $v_i$  and  $v_j$ . If there is no edge between  $v_i$  and  $v_j$ , the  $\mathbf{W}(i, j)$  is set to zero. The Laplacian matrix  $\mathbf{L}$  is defined as  $\mathbf{L} := \mathbf{D} - \mathbf{W}$ , where  $\mathbf{D}$  is a diagonal matrix containing the degree of each node.

Several studies have used the graph signal smoothness assumption to address graph inference problems. The discrete  $p$ -Dirichlet form has been introduced as a notion of global smoothness in such studies as those by [5], [15]:

$$S_p(\mathbf{x}) = \frac{1}{p} \sum_{i \in \mathcal{V}} \|\nabla_i \mathbf{x}\|_p^2. \quad (1)$$

For example, the well-known graph Laplacian quadratic form is achieved when  $p = 2$ :

$$S_2(\mathbf{x}) = \sum_{(i,j) \in \mathcal{E}} \mathbf{W}(i,j) [\mathbf{x}(j) - \mathbf{x}(i)]^2 = \mathbf{x}^T \mathbf{L} \mathbf{x}. \quad (2)$$

For multiple snapshots of graph signals, an extension of the graph Laplacian quadratic form can be expressed as:

$$S_2(\mathbf{X}) = \sum_{i=1}^m \mathbf{x}_i^T \mathbf{L} \mathbf{x}_i = \text{tr}(\mathbf{X}^T \mathbf{L} \mathbf{X}), \quad (3)$$

where  $\mathbf{x}_i \in \mathbb{R}^n$  represents a graph signal at time  $i$ ,  $m$  is the number of all available snapshots and  $\text{tr}(\cdot)$  denotes the trace operator.

### B. Graph Inference with Smooth Graph Signal Representation

The main objective of learning the graph structure based on smooth graph signal representation is to minimize the Laplacian quadratic function (3). However, minimizing this function (3) with respect to the Laplacian matrix ( $\mathbf{L}$ ) leads to the trivial solution of all edge weights being zero. To overcome this issue, regularization terms and constraints are introduced into the objective function [10] to estimate a valid  $\mathbf{L}$ :

$$\begin{aligned} \min_{\mathbf{L}} \quad & \text{tr}(\mathbf{X}^T \mathbf{L} \mathbf{X}) + \beta_1 \|\mathbf{L}\|_F^2 \\ \text{s.t.} \quad & \text{tr}(\mathbf{L}) = n, \\ & \mathbf{L}(i,j) = \mathbf{L}(j,i) \leq 0, \quad i \neq j, \\ & \mathbf{L} \mathbf{1} = \mathbf{0}, \end{aligned} \quad (4)$$

where,  $\beta_1$  is a regularization parameter,  $\mathbf{1}$  denotes the constant vector of ones, and  $\|\cdot\|_F$  represents the Frobenius norm of a matrix.

In [11], an alternative method was proposed for identifying a graph by exploring the space of weighted adjacency

matrices, instead of focusing solely on the Laplacian matrix. This approach leads to more straightforward and intuitive problem formulations, which can be solved more quickly and efficiently.

$$\begin{aligned} \min_{\mathbf{W}} \quad & \|\mathbf{W} \odot \mathbf{Z}\|_{1,1} - \alpha_2 \mathbf{1}^T \log(\mathbf{W} \mathbf{1}) + \frac{\beta_2}{2} \|\mathbf{W}\|_F^2 \\ \text{s.t.} \quad & \mathbf{W} \in \mathbb{R}_+^{n \times n}, \quad \mathbf{W} = \mathbf{W}^T, \quad \text{diag}(\mathbf{W}) = \mathbf{0}. \end{aligned} \quad (5)$$

The initial term represents the elementwise  $\ell_1$  norm, aimed at promoting sparsity. Here, the weights are determined by the distance between elements within the signal, generating a distance matrix  $\mathbf{Z}(i, j) = |\mathbf{x}(i) - \mathbf{x}(j)|^2$ . Additionally, the symbol  $\odot$  denotes the elementwise (Hadamard) product operation. The second term introduces a logarithmic barrier that enforces positive degrees but does not prevent individual edges from becoming zero.  $\alpha_2$  and  $\beta_2$  are the regularization parameters, and the space of solutions is restricted by constraints to enforce a positive edge weight, undirected graph, and graph without self-loop. In [11], this optimization problem (5) has been solved efficiently by primal-dual algorithms.

## III. PROPOSED METHODS

In this section, we first demonstrate how the characteristics of the physical processes in district heating networks can be interpreted as distances between nodes to construct a graph. Subsequently, we propose the informed graph learning (IGL) method by integrating this constructed graph into a smooth graph signal representation, enabling the learning of connections between nodes with limited domain knowledge. In summary, our approach learns a graph aligned with domain knowledge while leveraging smooth graph signal representation to uncover connections in less-explored areas.

### A. Physics-Inspired Graph Construction

Learning the graph, instead of relying solely on the physical connectivity of networks, offers several advantages. Firstly, physical connectivity graphs may not capture all relevant relationships and interactions among nodes, especially in complex systems where intricate dependencies exist. Moreover, they are less informative since they only indicate the connectivity without assigning any weights to the edges. This issue is particularly evident in our case study, which focuses on a district heating network. Despite the presence of physical connectivity, it may not comprehensively capture the complex interactions between nodes. However, this specific network has been studied from a fluid dynamics perspective. Therefore, an alternative approach to graph learning, as opposed to relying solely on physical connectivity, involves constructing a network graph based on available domain knowledge, interpreting certain characteristics of the physical processes as connectivity strengths between two nodes. District heating networks, typically equipped with pressure and temperature sensors for monitoring, can be represented as a graph by considering the variations in temperature and pressure drop along the pipes. Then, a stronger connection between the two sensors is established when there is a lower pressure and

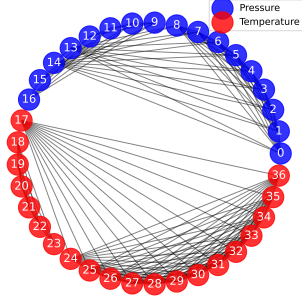


Fig. 1. Constructed graph based on characteristics of the physical processes.

temperature drop along the pipe between them. We calculate pressure drop ( $|\Delta P_{ij}|$ ) along two pressure nodes  $v_i$  and  $v_j$  by the Hazen-Williams equation as:

$$|\Delta P_{ij}| = \left| \frac{10.67 \cdot L_{ij} \cdot Q_{ij}^{1.852}}{R_{ij}^{1.852} \cdot D_{ij}^{4.87}} \right|, \quad (6)$$

where  $L_{ij}$ ,  $D_{ij}$ ,  $R_{ij}$ ,  $Q_{ij}$  represents the pipe length, diameter, Hazen-Williams roughness coefficient, and volumetric flow of the pipe which connects node  $v_i$  to  $v_j$ . The temperature drop ( $|\Delta T_{ij}|$ ) between node  $v_i$  and  $v_j$  can be approximated as:

$$|\Delta T_{ij}| \approx \left| \frac{\dot{q}_{ij}}{\dot{m}_{ij} \cdot C_{ij}} \right|, \quad (7)$$

where  $\dot{q}_{ij}$ ,  $C_{ij}$ ,  $\dot{m}_{ij}$  represent the heat transfer rate, the specific heat capacity of water, and mass flow rate, respectively.

After calculation of  $|\Delta P_{ij}|$  and  $|\Delta T_{ij}|$ , the graph can be constructed separately for each of the pressure ( $\mathbf{W}^p(i, j)$ ) and temperature sensors ( $\mathbf{W}^t(i, j)$ ) such that:

$$\mathbf{W}^p(i, j) = \frac{1}{|\Delta P_{ij}|}, \quad \mathbf{W}^t(i, j) = \frac{1}{|\Delta T_{ij}|}.$$

Since the values of temperature and pressure drops are in different ranges, we rescale  $\mathbf{W}^p(i, j)$  and  $\mathbf{W}^t(i, j)$  separately, such that the edge weights are between 0 and 1. Then, we eliminate edges with weights below 0.1 to enforce sparsity. Finally, to merge the scaled pressure graph ( $\mathbf{W}_s^p(i, j)$ ) and temperature graph ( $\mathbf{W}_s^t(i, j)$ ) into the overall physics-inspired graph ( $\mathbf{W}_{\text{PI}}$ ), we combine them into a block-diagonal matrix:

$$\mathbf{W}_{\text{PI}} = \begin{bmatrix} \mathbf{W}_s^p & \mathbf{0} \\ \mathbf{0} & \mathbf{W}_s^t \end{bmatrix}. \quad (8)$$

Equation (8) describes a unified graph that incorporates two distinct subgraphs, corresponding to pressure and temperature sensors, essentially forming two disconnected graphs within the larger structure. For better intuition, Figure 1 illustrates the graph constructed based on characteristics of the physical processes. It is evident that, due to the absence of domain knowledge connecting pressure to temperature nodes (or vice versa), the entire graph includes distinct subgraphs for each sensor type.

## B. Proposed Formulation for Informed Graph Learning

Once  $\mathbf{W}_{\text{PI}}$  is obtained based on domain knowledge, we can address a new optimization problem by incorporating additional regularization into Equation (5) to obtain the following:

$$\begin{aligned} \min_{\mathbf{W}} \quad & \|\mathbf{W} \odot \mathbf{Z}\|_{1,1} - \alpha \mathbf{1}^\top \log(\mathbf{W}\mathbf{1}) \\ & + \frac{\beta}{2} \|\mathbf{W}\|_F^2 + \frac{\nu}{2} \|\mathbf{M} \odot \mathbf{W} - \mathbf{W}_{\text{PI}}\|_F^2 \\ \text{s.t.} \quad & \mathbf{W} \in \mathbb{R}_+^{n \times n}, \quad \mathbf{W} = \mathbf{W}^\top, \quad \text{diag}(\mathbf{W}) = \mathbf{0}, \end{aligned} \quad (9)$$

where  $\mathbf{M}$  is the physical knowledge index matrix, indicating the links for which we have domain knowledge, such that:

$$\mathbf{M}(i, j) = \begin{cases} 1 & \mathbf{W}_{\text{PI}}(i, j) \neq 0 \\ 0 & \mathbf{W}_{\text{PI}}(i, j) = 0 \end{cases}. \quad (10)$$

Equation (9) specifies that the graph is learned with consideration for domain knowledge, as indicated by  $\mathbf{M}$ . The objective is to ensure consistency in the parts where domain knowledge is available ( $\mathbf{M}(i, j) = 1$ ). For the parts without domain knowledge ( $\mathbf{M}(i, j) = 0$ ), the goal is to rewire the graph using smooth graph signal representation. In summary, domain knowledge and smooth graph signal representation complement each other in the construction of a new graph, resulting in a graph signal that is both smooth and consistent with the provided domain knowledge.

## C. Optimization

The optimization problem specified in Equation (9) can be efficiently solved using various algorithms. Before deriving the update steps for this problem, it is essential to note that due to the symmetry of the matrix  $\mathbf{W}$  (second constraint) and the absence of self-loops (third constraint), the problem can be effectively solved by focusing solely on the upper triangular part of  $(\mathbf{W}(i, j), j > i)$ . This implies that instead of addressing the problem in  $\mathbb{R}_+^{n \times n}$ , it can be tackled in  $\mathbf{w} \in \mathbb{R}_+^{n(n-1)/2}$  without explicit consideration of the second and third constraints. Additionally, similar to [11], we incorporate an indicator function ( $\mathbb{1}\{\mathbf{w} \succeq \mathbf{0}\} = 0$  if  $\mathbf{w} \succeq \mathbf{0}$ , and  $\mathbb{1}\{\mathbf{w} \succeq \mathbf{0}\} = \infty$  otherwise) as a penalty function to enforce non-negativity constraints. With these definitions, we reformulate the objective in equation (9) as:

$$\begin{aligned} \min_{\mathbf{w}} \quad & (\mathbb{1}\{\mathbf{w} \succeq \mathbf{0}\} + 2\mathbf{w}^\top \mathbf{z} - \alpha \mathbf{1}^\top \log(\mathbf{d}) \\ & + \beta \|\mathbf{w}\|^2 + \nu \|\mathbf{m} \odot \mathbf{w} - \mathbf{w}_{\text{PI}}\|^2), \end{aligned} \quad (11)$$

where  $\mathbf{d} \in \mathbb{R}_+^n$  represents the vector of node degrees. To adapt the optimization problem (11) for primal-dual algorithms [16], we divide the objective into the sum of three functions to utilize the Monotone+Lipschitz Forward Backward Forward (M+LFBF) algorithm:

$$\min_{\mathbf{w}} f(\mathbf{w}) + g(\mathbf{S}\mathbf{w}) + h(\mathbf{w}), \quad (12)$$

where  $h$  is required to be differentiable with a gradient that possesses a Lipschitz constant  $\zeta$ . The functions  $f$  and  $g$  should

be such that their proximal operators are readily accessible. Owing to  $\mathbf{S}$  being a linear operator,  $g$  is defined on the dual variable ( $\mathbf{S}\mathbf{w} = \mathbf{d} = \mathbf{W}\mathbf{1} \in \mathbb{R}^n$ ). Finally, based on (11) and (12), we can delineate and define  $f$ ,  $g$ , and  $h$  in the following way:

$$f(\mathbf{w}) = \mathbb{1}\{\mathbf{w} \succeq \mathbf{0}\} + 2\mathbf{w}^\top \mathbf{z}, \quad (13)$$

$$g(\mathbf{d}) = -\alpha \mathbf{1}^\top \log(\mathbf{d}), \quad (14)$$

$$h(\mathbf{w}) = \beta \|\mathbf{w}\|^2 + v \|\mathbf{m} \odot \mathbf{w} - \mathbf{w}_{\text{PI}}\|^2 \quad \zeta = 2(\beta + v). \quad (15)$$

Finally, to derive the optimization step, we have:

$$\text{prox}_{\lambda f}(\mathbf{y}) = \max(\mathbf{0}, \mathbf{y} - \lambda \mathbf{z}), \quad \text{elementwise} \quad (16)$$

$$\text{prox}_{\lambda g}(\mathbf{y}) = \frac{\mathbf{y} + \sqrt{\mathbf{y}^2 + 4\alpha\lambda}}{2}, \quad \text{elementwise} \quad (17)$$

$$\nabla h(\mathbf{w}) = 2\beta\mathbf{w} + 2v(\mathbf{m} \odot \mathbf{w} - \mathbf{w}_{\text{PI}}). \quad (18)$$

Algorithm 1 provides a comprehensive summary of the informed graph learning (IGL) method.

---

**Algorithm 1:** M+LFBF Algorithm for IGL (11)

---

**Input** :  $\alpha, \beta, \gamma \in (0, 1 + \zeta + \|\mathbf{S}\|)$ ,  $v, \epsilon_0, \mathbf{z}, \mathbf{S}, \mathbf{m}, \mathbf{w}_{\text{PI}}$   
**Initialize:**  $\mathbf{w}^0 \in \mathbb{R}_+^{n(n-1)/2}$ ,  $\mathbf{d}^0 \in \mathbb{R}_+^n$   
**for**  $k = 1, \dots, k_{\text{max}}$  **do**  
     $\mathbf{y}^k = \mathbf{w}^k - \gamma(2\beta\mathbf{w}^k + 2v(\mathbf{m} \odot \mathbf{w}^k - \mathbf{w}_{\text{PI}}) + \mathbf{S}^\top \mathbf{d}^k)$ ;  
     $\bar{\mathbf{y}}^k = \mathbf{d}^k + \gamma(\mathbf{S}\mathbf{w}^k)$ ;  
     $\mathbf{p}^k = \max(\mathbf{0}, \bar{\mathbf{y}}^k - 2\gamma\mathbf{z})$  # elementwise;  
     $\bar{\mathbf{p}}^k = (\bar{\mathbf{y}}^k - \sqrt{(\bar{\mathbf{y}}^k)^2 + 4\alpha\gamma})/2$  # elementwise;  
     $\mathbf{q}^k = \mathbf{p}^k - \gamma(2\beta\mathbf{p}^k + 2v(\mathbf{m} \odot \mathbf{p}^k - \mathbf{w}_{\text{PI}}) + \mathbf{S}^\top \mathbf{p}^k)$ ;  
     $\bar{\mathbf{q}}^k = \bar{\mathbf{p}}^k + \gamma(\mathbf{S}\mathbf{p}^k)$ ;  
     $\mathbf{w}^k = \mathbf{w}^k - \mathbf{y}^k + \mathbf{p}^k$ ;  
     $\mathbf{d}^k = \mathbf{d}^k - \bar{\mathbf{y}}^k + \bar{\mathbf{q}}^k$ ;  
    **if**  $\frac{\|\mathbf{w}^k - \mathbf{w}^{k-1}\|}{\|\mathbf{w}^{k-1}\|} < \epsilon_0$  **and**  $\frac{\|\mathbf{d}^k - \mathbf{d}^{k-1}\|}{\|\mathbf{d}^{k-1}\|} < \epsilon_0$  **then**  
        **break**;  
**Output** :  $\mathbf{w}^k$

---

After solving the problem for the upper triangular part of the weighted adjacency matrix through vectorization, we can reconstruct the symmetric adjacency matrix  $\mathbf{W}$ . The complexity of Algorithm 1 is  $\mathcal{O}(n^2)$  for each iteration with  $n$  nodes, and it can be executed in parallel.

#### IV. EXPERIMENTAL RESULTS

Due to the absence of publicly available real-world datasets for district heating networks, we have created a synthetic dataset consisting of 8760 samples, using the TesPy library [17] for this purpose. The first 5000 samples are allocated for training, while the remaining 3760 samples are used for testing. Min-max normalization is applied separately to pressure and temperature sensors, based on the minimum and maximum values of the training set. To enhance the realism of the synthetic dataset, zero-mean Gaussian noise with a standard deviation ( $\sigma$ ) of 0.25 is added to the training data.

TABLE I  
QUANTITATIVE COMPARISON OF METHODS FOR GRAPH SIGNAL RECONSTRUCTION

Scenario	Metric	Physics	Lap-Smooth	Adj-Smooth	IGL
Denoising ( $\sigma = 0.3$ )	RMSE	2.829	2.421	2.403	<b>2.395</b>
	MAE	1.716	1.475	1.466	<b>1.460</b>
Imputation ( $\rho = 0.3$ )	RMSE	5.761	2.164	1.824	<b>1.813</b>
	MAE	1.888	1.179	0.987	<b>0.977</b>
Imputation ( $\rho = 0.5$ )	RMSE	2.558	1.846	1.489	<b>1.466</b>
	MAE	1.056	1.091	0.885	<b>0.869</b>
Imputation ( $\rho = 0.7$ )	RMSE	1.567	1.774	1.425	<b>1.393</b>
	MAE	0.911	1.055	0.846	<b>0.824</b>
Imputation ( $\rho = 0.9$ )	RMSE	1.516	1.746	1.400	<b>1.359</b>
	MAE	0.909	1.049	0.836	<b>0.808</b>

For hyperparameter tuning, 5-fold cross-validation is employed on the training data to select the optimal parameters based on denoising performance<sup>1</sup>.

For comparison, we evaluate our proposed IGL algorithm against a pure domain knowledge approach (8) based on characteristics of the physical processes, referred to as ‘Physics’ in the results, smoothness optimization on the Laplacian matrix, referred to as Lap-Smooth [10], and smoothness optimization on the adjacency matrix, referred to as Adj-Smooth [11]. For evaluation, the learned graph from each method is utilized in denoising and imputation tasks by solving the convex optimization problem in the Appendix. For denoising, zero-mean Gaussian noise with a standard deviation of 0.3 is added to the test data. Additionally, four different cases related to various sampling densities ( $\rho$ ) are considered for missing data imputation, where  $\rho$  represents the fraction of available sensor data measurements. The evaluation metrics for both tasks include root-mean-square error (RMSE) and mean absolute error (MAE). Table I presents the results for both imputation and denoising tasks. It can be observed that the graph constructed based on the underlying physics exhibits a significant performance drop as the number of missing values increases (for  $\rho = 0.3$  and 0.5). However, its performance remains competitive compared to other methods as the sampling ratio increases, attributed to the graph’s limitation of considering only similar sensor types. This limitation prevents it from capturing complex interactions among different sensor types, thus hindering its effectiveness in scenarios of low sampling densities. Moreover, the performance of Adj-Smooth and the proposed IGL method shows strong competitiveness. However, at higher sampling ratios ( $\rho = 0.7$  and 0.9) for the imputation task, the performance gap widens, with the proposed IGL method outperforming Adj-Smooth. This advantage comes from the additional regularization proposed, inspired by the characteristics of physical processes in district heating networks. For a more comprehensive comparison, the absolute difference between adjacency matrices of IGL and Adj-Smooth is visually represented by colormap in Fig. 2.

<sup>1</sup> $\beta = 0.4$  captures edge density patterns, and  $v = 0.4$  signifies the fidelity of the learned graph to domain knowledge. The optimization stopping criterion,  $\epsilon_0$ , is set to  $10^{-5}$ . Moreover, the learned adjacency matrix is normalized through elementwise division of each entry by the maximum edge value, followed by thresholding to drop weak edges with values less than 0.1.

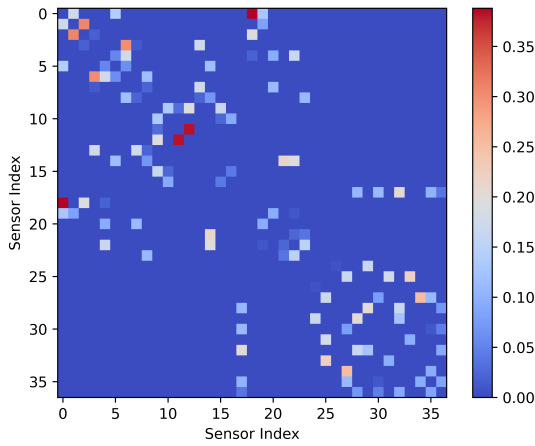


Fig. 2. Colormap showing the absolute difference between IGL and Adj-Smooth adjacency matrices. Nodes 0-16 are pressure sensors, and nodes 17-36 are temperature sensors.

## V. CONCLUSION

This study proposes a novel method for informed graph learning by using the characteristics of the physical processes in district heating networks and smooth graph signal representation. The efficacy of the proposed approach was demonstrated through graph signal reconstruction, resulting in performance improvement relative to the compared methods. To the best of our knowledge, this work represents the first exploration of GSP in district heating networks. The proposed method can also be applied to other networks, such as power grids, where the graph can be constructed based on voltage drops among nodes. Future research directions may include assessing the proposed method in other tasks. In summary, the insights presented in this paper contribute to the progress of interdisciplinary research in signal processing.

## APPENDIX

### A. Graph Signal Reconstruction

Following graph inference, various inverse problems for graph signals can be addressed. Our emphasis in this study lies in the denoising and imputation. Specifically, for denoising purposes, the optimization problem takes the form:

$$\min_{\mathbf{X}} \|\mathbf{Y} - \mathbf{X}\|_F^2 + \mu \text{tr}(\mathbf{X}^T \mathbf{L} \mathbf{X}), \quad (19)$$

where  $\mathbf{Y}$  is noisy data observation. Remarkably, a closed-form solution exists for this optimization problem, which is:

$$\mathbf{X} = (\mathbf{I} + \mu \mathbf{L})^{-1} \mathbf{Y}. \quad (20)$$

Since the matrix  $\mathbf{I} + \mu \mathbf{L}$  is positive definite, the inverse of this matrix can be efficiently computed through Cholesky decomposition [10], [18].

For graph signal imputation, one can solve the following optimization problem:

$$\min_{\mathbf{X}} \frac{1}{2} \text{tr}(\mathbf{X}^T \mathbf{L} \mathbf{X}) \quad \text{s.t.} \quad \mathbf{J} \odot \mathbf{X} = \mathbf{Y}, \quad (21)$$

where  $\mathbf{Y}$  is our observation with some missing values caused by sampling matrix  $\mathbf{J}$ . The solution to this problem (21) can be achieved through the gradient projection algorithm with the following iterative update:

$$\mathbf{X}^{k+1} = \mathcal{P}_{\mathbf{Y}} (\mathbf{X}^k - \xi \nabla_{\mathbf{X}} f_n(\mathbf{X}^k)), \quad (22)$$

where  $f_n(\mathbf{X}^k) = \frac{1}{2} \text{tr}((\mathbf{X}^k)^T \mathbf{L} \mathbf{X}^k)$ ,  $\xi$  is the step size,  $\nabla_{\mathbf{X}} f_n(\mathbf{X}^k)$  is the gradient of the function  $f_n(\mathbf{X}^k)$  given by

$$\nabla_{\mathbf{X}} f_n(\mathbf{X}^k) = \mathbf{L} \mathbf{X}^k, \quad (23)$$

and  $\mathcal{P}_{\mathbf{Y}}(\mathbf{A})$  is the projection of  $\mathbf{A}$  to space  $\mathbf{Y}$  given by  $\mathcal{P}_{\mathbf{Y}}(\mathbf{A}) = \mathbf{Y} + \mathbf{A} - \mathbf{J} \odot \mathbf{A}$ .

## REFERENCES

- [1] K.-H. N. Bui, J. Cho, and H. Yi, "Spatial-temporal graph neural network for traffic forecasting: An overview and open research issues," *Appl. Intell.*, vol. 52, no. 3, pp. 2763–2774, 2022.
- [2] K. F. Niresi, M. Zhao, H. Bissig, H. Baumann, and O. Fink, "Spatial-temporal graph attention fuser for calibration in iot air pollution monitoring systems," in *Proc. IEEE SENSORS*, 2023.
- [3] R. Li, X. Yuan, M. Radfar, P. Marendy, W. Ni, T. J. O'Brien, and P. M. Casillas-Espinosa, "Graph signal processing, graph neural network and graph learning on biological data: A systematic review," *IEEE Rev. Biomed. Eng.*, vol. 16, pp. 109–135, 2023.
- [4] A. Ortega, P. Frossard, J. Kováčević, J. M. Moura, and P. Vandergheynst, "Graph signal processing: Overview, challenges, and applications," *Proc. IEEE*, vol. 106, no. 5, pp. 808–828, 2018.
- [5] D. I. Shuman, S. K. Narang, P. Frossard, A. Ortega, and P. Vandergheynst, "The emerging field of signal processing on graphs: Extending high-dimensional data analysis to networks and other irregular domains," *IEEE Signal Process. Mag.*, vol. 30, no. 3, pp. 83–98, 2013.
- [6] C. Shang, J. Chen, and J. Bi, "Discrete graph structure learning for forecasting multiple time series," in *Proc. Int. Conf. Learn. Representations (ICLR)*, 2021.
- [7] V. Matta, A. Santos, and A. H. Sayed, "Graph learning under partial observability," *Proc. IEEE*, vol. 108, no. 11, pp. 2049–2066, 2020.
- [8] L. Qiao, L. Zhang, S. Chen, and D. Shen, "Data-driven graph construction and graph learning: A review," *Neurocomputing*, vol. 312, pp. 336–351, 2018.
- [9] X. Dong, D. Thanou, M. Rabbat, and P. Frossard, "Learning graphs from data: A signal representation perspective," *IEEE Signal Process. Mag.*, vol. 36, no. 3, pp. 44–63, 2019.
- [10] X. Dong, D. Thanou, P. Frossard, and P. Vandergheynst, "Learning laplacian matrix in smooth graph signal representations," *IEEE Trans. Signal Process.*, vol. 64, no. 23, pp. 6160–6173, 2016.
- [11] V. Kalofolias, "How to learn a graph from smooth signals," in *Proc. Int. Conf. Artif. Intell. Statist.*, 2016, pp. 920–929.
- [12] D. Thanou, X. Dong, D. Kressner, and P. Frossard, "Learning heat diffusion graphs," *IEEE Trans. Signal Inf. Process. Netw.*, vol. 3, no. 3, pp. 484–499, 2017.
- [13] S. Segarra, A. G. Marques, G. Mateos, and A. Ribeiro, "Network topology inference from spectral templates," *IEEE Trans. Signal Inf. Process. Netw.*, vol. 3, no. 3, pp. 467–483, 2017.
- [14] G. Mateos, S. Segarra, A. G. Marques, and A. Ribeiro, "Connecting the dots: Identifying network structure via graph signal processing," *IEEE Signal Process. Mag.*, vol. 36, no. 3, pp. 16–43, 2019.
- [15] J. H. Giraldo, A. Mahmood, B. Garcia-Garcia, D. Thanou, and T. Bouwmans, "Reconstruction of time-varying graph signals via sobolev smoothness," *IEEE Trans. Signal Inf. Process. Netw.*, vol. 8, pp. 201–214, 2022.
- [16] N. Komodakis and J.-C. Pesquet, "Playing with duality: An overview of recent primal? dual approaches for solving large-scale optimization problems," *IEEE Signal Process. Mag.*, vol. 32, no. 6, pp. 31–54, 2015.
- [17] F. Witte and I. Tuschy, "TESPy: Thermal Engineering Systems in Python," *J. Open Source Softw.*, vol. 5, no. 49, p. 2178, 2020.
- [18] S. P. Boyd and L. Vandenberghe, *Convex Optimization*. Cambridge University Press, 2004.